

The Cerebellar Development in Chinese Children—A Study by Voxel-Based Volume Measurement of Reconstructed 3D MRI Scan

KUAN-HSUN WU, CHIA-YUAN CHEN, AND EIN-YIAO SHEN

Departments of Pediatrics [K.-H.W.] and Radiology [C.-Y.C.], Taipei Medical University, Wan Fang Hospital, Taipei 116, Taiwan; Graduate Institute of Acupuncture Science [E.-Y.S.], China Medical University, Taichung 404, Taiwan; Department of Pediatrics [E.-Y.S.], China Medical University Hospital, Taipei Branch, Taipei 114, Taiwan

ABSTRACT: Cerebellar disorder was frequently reported to have relation with structural brain volume alteration and/or morphology change. In dealing with such clinical situations, we need a convenient and noninvasive imaging tool to provide clinicians with a means of tracing developmental changes in the cerebellum. Herein, we present a new daily practice method for cerebellum imaging that uses a work station and a software program to process reconstructed 3D neuroimages after MRI scanning. In a 3-y period, 3D neuroimages reconstructed from MRI scans of 50 children aged 0.2–12.7 y were taken. The resulting images were then statistically analyzed against a growth curve. We observed a remarkable increase in the size of the cerebellum in the first 2 y of life. Furthermore, the unmyelinated cerebellum grew mainly between birth and 2 y of age in the postnatal stage. In contrast, the postnatal development of the brain mainly depended on the growth of myelinated cerebellum from birth through adolescence. This study presents basic data from a study of ethnic Chinese children's cerebellums using reconstructed 3D brain images. Based on the technique we introduce here, clinicians can evaluate the growth of the brain. (*Pediatr Res* 69: 80–83, 2011)

Brain development in early life is thought to be more susceptible to injury than in the latter stages. Any insult at this stage can cause permanent injury resulting in disability, which is different from a mature cerebellum's injury that might be restored partially by rehabilitation. The previous literature of studies of the cerebellum clarified relationships between structural brain volume alterations and symptoms in various regions (1–4). Furthermore, based on a report by Krägeloh-Mann *et al.* (5), marked cerebellar atrophy in pre-term babies was considered to be related to severe developmental delays. Thus, cerebellar atrophy was shown to be a bad prognostic factor of motor and cognitive outcomes in children.

In our daily pediatric neurology practice, we need a imaging tool to provide clinicians with the ability to trace developmental changes in the cerebellum of children and provide a reliable data reference base for healthy children. It would be helpful for interpreting information and communicating with the patients and their family.

Herein, we present a new method for 3D image reconstruction using a conventional MRI scanner connected to a workstation. After carefully setting up the parameters for MRI

scanning, the reconstruction process was managed by a software program that uses data from the MRI scanner. With this technique, we were able to study cerebellar growth in children with volume measurements from reconstructed 3D images of the brain. Few studies outside the United States and Europe have systematically examined cerebellar development in childhood (6), and there are no detailed cerebellum development data for ethnic Chinese children. The purpose of this study was to establish such a database for further study.

METHODS

Patients. We collected data on subjects for a 3-y period at the Department of Pediatrics, Wan-Fang Hospital, Taipei, Taiwan. Data were obtained from subjects undergoing ordinary health examinations or other reasons for which neurologist had suggested an MRI brain imaging study, except those who had any form of cerebellar dysfunction. Those suggested for further MRI study included paroxysmal disorders or functional disorders, such as headache, Tourette syndrome, autism, seizure, and so on. Brain MRI studies were applied to each of them followed by a 3D neuroimaging reconstruction processing study. If the subjects were later diagnosed as having cerebellar disease, then they were excluded from the study. In total, 50 cases were included during this period. All work performed in this study was approved by the ethics committee of Wan-Fang Hospital. Informed consent was obtained from all patients or a parent before study participation.

Technique for 3D reconstruction. We performed this process of 3D reconstruction according to Schierlitz *et al.* (7) using 2D medical images and Avizo software (Version 5.1; Mercury Computer Systems, Inc., Germany). The method for 3D image reconstruction began by setting up the indicator for MRI scanning to a mode suitable for large datasets that can work well on personal computers (PCs) using the Avizo software. A GE 1.5 excite machine is used in this hospital. A subject's brain was scanned using transverse planes of ≤ 1.5 mm to obtain at least 80–120 slices. The conditions for MRI scanning were as follows: 1) patient position: supine, 2) coil: head, 3) T1W: 3D SPGR, 4) TR: 33, 5) TE: 3.0, 6) flip angle: 35°, 7) bandwidth: 15.63, 8) matrix: 256 × 192 zip 512, 9) field of vision (Fov): 22 cm, and 10) cover range: whole brain. Scans were collected for algorithmic reconstruction and transmitted from the MR unit database to an established workstation. The 3D Avizo software system was then used for image processing. The skull component of the brain was visually removed from the regions of interest using an arithmetic module to isolate the cerebellar hemisphere. We limited gray-scale values to 110–155 of 1024 (2^{10}) scales to approximate the boundary of the unmyelinated cerebellum. The software's "threshold" and "edge detection" tools allowed the unmyelinated cerebellum to be precisely delineated. Certain areas with fewer than 50 pixels (area < 0.1 cm²) were removed to eliminate erroneously identified unmyelinated cerebellum. We then repeated the procedure for the myelinated cerebellum with gray-scale values in the range of 75–95 of 1024. Subsequently, we computed volumetric measurements of the unmyelinated cerebellum with the following formula: volume of cortex = (number of voxels within the cortex) × (volume per voxel), derived from the formula of Courchesne *et al.* (8), which can be modified to compute the myelinated cerebellum and entire cerebellar volumes. These procedures were done by a technician and a physician concurrently for three times to minimize the human operational errors and reconfirm the areas classified.

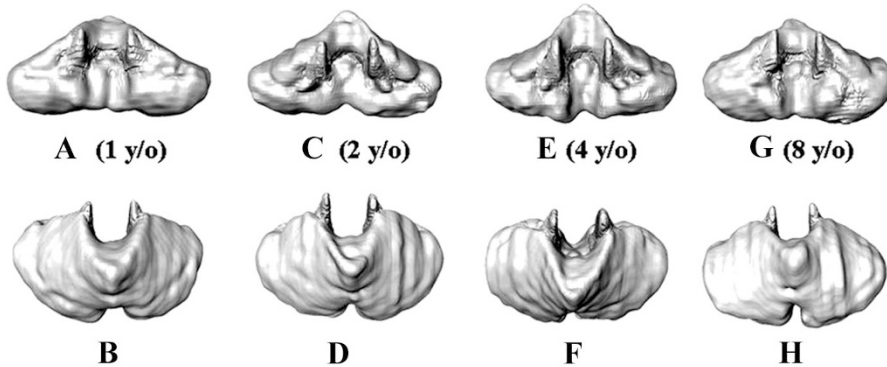
Reliability of regional volumetric measurements. Interrater reliability was examined in a sample of 20 randomly selected brain scans analyzed by two raters

Received February 26, 2010; accepted August 28, 2010.

Correspondence: Ein-Yiao Shen, M.D., Department of Pediatrics, China Medical University Hospital, Taipei Branch, No. 360, Sec. 2, Neihu Road, Neihu District, Taipei City 114, Taiwan; e-mail: einyiao@gmail.com

Table 1. The unmyelinated, myelinated, and total cerebellar volume by 50 aged patients

Group	Sex (M:F)	Age	N	Unmyelinated cerebellar volume (cm ³)		Myelinated cerebellar volume (cm ³)		Total cerebellar volume (cm ³)	
				Range	Mean ± SD	Range	Mean ± SD	Range	Mean ± SD
1	2:3	3–11 mo	5	35.4–107.3	67.8 ± 25.9	5.3–17.6	9.7 ± 4.9	40.6–124.9	77.5 ± 30.3
2	4:1	1–1.9 y	5	78.4–109.3	91.5 ± 16.1	9.9–17.6	13.2 ± 3.1	91.7–126.6	104.7 ± 17.2
3	2:2	2–3.9 y	4	81.3–114.1	96.8 ± 13.9	10.4–23.3	17.1 ± 5.2	91.7–131.7	113.9 ± 17.6
4	13:5	4–5.9 y	18	74.4–113.0	93.9 ± 10.3	12.8–28.7	19.6 ± 4.9	91.8–139.7	113.6 ± 12.2
5	7:2	6–8.9 y	9	52.9–105.5	89.3 ± 15.2	13.7–40.9	26.8 ± 8.9	66.7–139.8	116.1 ± 21.2
6	6:3	9–12 y	9	70.1–109.1	92.4 ± 16.8	16.1–34.1	23.4 ± 6.1	86.2–138.1	115.8 ± 19.9

Figure 1. 3D reconstructed neuroimages of the cerebellum at different ages are as follows: (A) anterior view, (B) vertical view of a 1-y-old child (volume: 79.12 cm³); (C) anterior view, (D) vertical view of a 2-y-old child (volume: 91.44 cm³); (E) anterior view, (F) vertical view of a 4-y-old child (volume: 92.27 cm³); and (G) anterior view, (H) vertical view of an 8-y-old child (volume: 102.52 cm³).

(K.-H.W. and C.-Y.C.). The intraclass correlation for total cerebellum volumes ranged from 0.93 to 0.95 and those of myelinated and unmyelinated volumes from 0.90 to 0.92. The intrarater reliability was also examined in the same 20 scans analyzed by one of these raters (K.-H.W.), and the correlation for total cerebellum, myelinated, and unmyelinated volumes ranged from 0.94 to 0.97. The rater (K.-H.W.) then completed the analysis on the remaining scans.

Statistical analysis. We conducted statistical analyses of the data with Excel 2003 and SPSS version 11.5. The total cerebellar volume, which was further differentiated into unmyelinated and myelinated cerebellum, was recorded by age and gender. The regression curves were individually graphed, and equations were determined. Our statistical probabilities and regression analyses used logarithmic functions.

RESULTS

During a 3-y period, we collected 50 cases that were enrolled in this study. The gender, age distribution, and unmyelinated, myelinated, and total cerebellar volume are given in Table 1. There are two preterm births in this study (in Taiwan, the definition of full-term babies is around 38–40 wk of postconceptual age): one was born at 36th wk with the birth weight of 3100 g, MRI was done at 9 mo and 27 d postnatal, hence the adjusted postnatal age for this infant was 9 mo; another one was born at 35th wk and had the MRI done at 2 mo and 25 d, hence the age was adjusted to 2 mo. In the research processes, all ages were adjusted, and all the parameters examined were within normal ranges, *i.e.* birth weights were between 2500 and 4000 g, birth heights were between 45 and 55 cm, head circumferences were between 34 and 38 cm, and all were within 3–97 percentile of normal range. The evaluations of whole cerebellar volume by radiologist and cerebellar function by neurologist also showed that there were no abnormal cases. Reconstructed 3D images of cerebellar growth of selected stages are shown in Figure 1. As Figure 2 shows, the regression curve of normal cerebellar growth at the ages of 0.2–12.7 y was $y = 12.743Ln(x) + 91.562$, $r^2 = 0.313$, and the regression curve for the normal growth of unmyelinated cerebellum was $y = 7.3662Ln(x) + 79.583$,

$r^2 = 0.1695$, and normal growth of myelinated cerebellum was $y = 5.3797Ln(x) + 11.974$, $r^2 = 0.4166$ (Fig. 2). In the formula, y is the volume and x the mean age. It is evident that the cerebellum volume substantially increased in the first 2 y of life. The majority of the cerebellar volume was accounted for by unmyelinated cerebellum, which increased by almost 130% in the first 2 y; myelinated cerebellar volume also obviously increased in the first 2 y. The ratio of the volumes of unmyelinated to myelinated cerebellum after 2 y old was ~4:1. When we considered the gender factor in the analysis, the volume of cerebellar growth differed between females and males, with girls always lagging behind; it is not until ~12 y of age that they had caught up to the volume of the male cerebellum (Fig. 3A). We also determined the male cerebellum growth equation to be $y = 6.6346Ln(x) + 104.66$, $r^2 = 0.0866$ and the equation for females to be $y = 16.625Ln(x) + 79.581$, $r^2 = 0.6881$ (Fig. 3A). Furthermore, as Figure 3B shows, it is evident that the volume of myelinated cerebellum increased with age, increasing more in females than in males, although the male myelinated cerebellar volume was greater than that of females in the infant stage. The male myelinated cerebellum growth equation was $y = 4.4506Ln(x) + 13.613$, $r^2 = 0.2485$ and that of females was $y = 6.0392Ln(x) + 10.881$, $r^2 = 0.6485$. However, the male unmyelinated cerebellar volume began to level off after 2 y old and was greater than that of females until around 11 y old, despite the rapidly increasing volume of females (Fig. 3C).

DISCUSSION

The advancement of digital image processing with algorithms makes it possible to practically, effectively, and efficiently demonstrate 3D images. Our study used a high-resolution gray-scale (1024) method to define gray-scale levels of different parts of the brain on a delicately sliced MRI

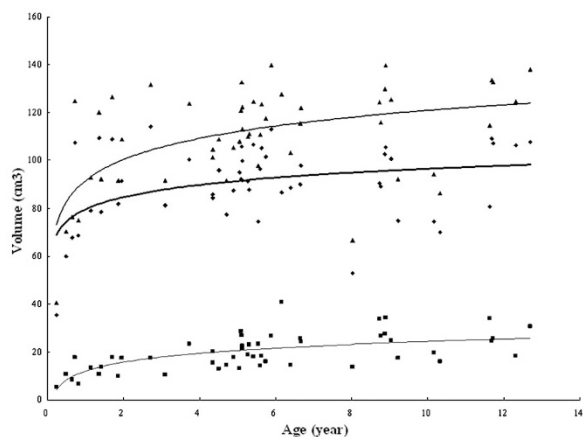


Figure 2. Growth curves of the total cerebellum, unmyelinated, and myelinated cerebellar volume (cm^3) from 3 mo to 12.7 y of per age group; \blacktriangle means of unmyelinated cerebellum, \blacksquare means of myelinated cerebellum, and \blacktriangle means of cerebellum. The regression curve of normal cerebellar growth at the ages of 0.2–12.7 y was $y = 12.743\text{Ln}(x) + 91.562$, $r^2 = 0.313$, and the regression curve for the normal growth of unmyelinated cerebellum was $y = 7.3662\text{Ln}(x) + 79.583$, $r^2 = 0.1695$ and normal growth of myelinated cerebellum was $y = 5.3797\text{Ln}(x) + 11.974$, $r^2 = 0.4166$. In the formula, y represents volume and x represents age.

scan (slice thickness of 1.5 mm, with ~ 80 –120 slices in a normal brain). Then, we setup a level threshold and processed the images digitally. With this procedure, we can display each component of the brain using 3D images, including the cortex, myelinated brain tissue, ventricles, vessels, and pathological lesions. With delicately sliced MRI scans, this technology can become a new tool for more-precisely demonstrating both the normal anatomy and pathological lesions of the brain. This program can also be modified to perform volume arithmetic, which enables the evaluation of brain volume. Computation of volumetric measurements of the unmyelinated cerebellum used the following formula: volume of the cortex = (number of voxels within the cortex) \times (volume per voxel). Modifications to this formula can allow computation of the volume of the myelinated cerebellum, ventricles, whole brain, and even brain lesions (8).

Brain development in early childhood is extremely dynamic and is thought to be critical in neurodevelopmental disorders. Quantitative MRI has significantly advanced our understanding of brain development during growth. Several large-scale longitudinal studies have been published (6,9). However, none of those large-scale studies focused on the cerebellum or covered the age from infancy to adolescent. Filling in this serious gap in our current knowledge was one of the motivations to perform this study.

Cerebellar growth in our study possessed a similar trend to that of the cerebrum, which was reported previously (10–16). We observed a dramatic increase in the size of the cerebellum in the first 2 y of life, in which overall unmyelinated cerebellar volumes rapidly increased to a lifetime maximum at around age 2 y (Fig. 3C), and myelinated cerebellum continually increased beyond childhood (Fig. 3B).

Giedd *et al.* (9) had reported that volume changes of cerebrum cortical gray matter were nonlinear and regionally specific, but grew with the similar pattern that they increased

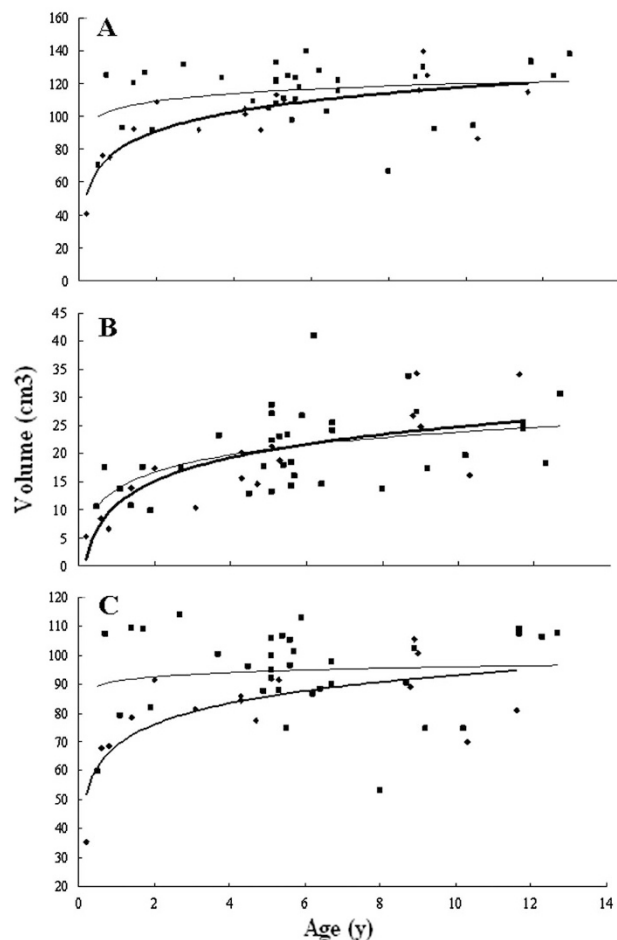


Figure 3. Growth curves of the cerebellum of male and female children from 3 mo to 12.7 y of age. \blacktriangle means of female and \blacksquare means of male. (A) Growth curves of the cerebellum of male was $y = 6.6346\text{Ln}(x) + 104.66$, $r^2 = 0.0866$ and female was $y = 16.625\text{Ln}(x) + 79.581$, $r^2 = 0.6881$. (B) Growth curves of the myelinated cerebellum of male was $y = 4.4506\text{Ln}(x) + 13.613$, $r^2 = 0.2485$ and female was $y = 6.0392\text{Ln}(x) + 10.881$, $r^2 = 0.6485$. (C) Growth curves of the unmyelinated cerebellum of male was $y = 2.1892\text{Ln}(x) + 91.032$, $r^2 = 0.0136$ and female was $y = 10.587\text{Ln}(x) + 68.696$, $r^2 = 0.5731$. In the formula, y represents volume and x represents age.

during preadolescence with a maximum size, followed by a decline during postadolescence. This phenomenon was not seen in our result of unmyelinated cerebellum growth. The volume of unmyelinated cerebellum increased as a sharply parabolic curve with age, increasing less in females than in males, and became leveling beyond ~ 12 y old.

Another recent report using quantitative diffusion tensor imaging to evaluate cerebellar white matter development also demonstrated that myelination of the cerebellar white matter continued to sharply increase for up to 36 mo after birth, which was then followed by a gradual increase into childhood and adolescence (17). As myelination and synapse formation account for brain and white matter growth during the postnatal stage, these also support our finding of continual increases in the myelinated cerebellar volume.

Interestingly, when we analyzed the data differentiated by gender, female children seemed to lag behind males in development. We do not know whether this result is because of the

limited study number or not. We believe that in the future, after more data become available, this condition will be elucidated.

Accumulating evidence reveals that cerebellar growth may underpin motor and cognitive development in infancy (18–20). Many cerebellar disorders are frequently reported to be related to structural brain volume alterations and/or morphological changes (1–4). Our quantitative information on cerebellar development may play a pivotal role in clarifying brain neurodevelopmental abnormalities. Also, this 3D neuroimaging method could serve clinicians as a way to visualize and to study brain development in patients, which might be helpful for physicians to communicate information to the patients and their family.

REFERENCES

1. Mostofsky SH, Mazzocco MM, Aakalu G, Warsofsky IS, Denckla MB, Reiss AL 1998 Decreased cerebellar posterior vermis size in fragile X syndrome: correlation with neurocognitive performance. *Neurology* 50:121–130
2. Pinter JD, Eliez S, Schmitt JE, Capone GT, Reiss AL 2001 Neuroanatomy of Down's syndrome: a high-resolution MRI study. *Am J Psychiatry* 158:1659–1665
3. Berquin PC, Giedd JN, Jacobsen LK, Hamburger SD, Krain AL, Rapoport JL, Castellanos FX 1998 Cerebellum in attention-deficit hyperactivity disorder: a morphometric MRI study. *Neurology* 50:1087–1093
4. Kułak W, Sobaniec W 2007 Magnetic resonance imaging of the cerebellum and brain stem in children with cerebral palsy. *Adv Med Sci* 52:180–182
5. Krägeloh-Mann I, Toft P, Lunding J, Andresen J, Pryds O, Lou HC 1999 Brain lesions in preterms: origin, consequences and compensation. *Acta Paediatr* 88:897–908
6. Sowell ER, Thompson PM, Leonard CM, Welcome SE, Kan E, Toga AW 2004 Longitudinal mapping of cortical thickness and brain growth in normal children. *J Neurosci* 24:8223–8231
7. Schierlitz L, Dumanli H, Robinson JN, Burrows PE, Schreyer AG, Kikinis R, Jolesz FA, Tempny CM 2001 Three-dimensional magnetic resonance imaging of fetal brains. *Lancet* 357:1177–1178
8. Courchesne E, Chisum HJ, Townsend J, Cowles A, Covington J, Egaas B, Harwood M, Hinds S, Press GA 2000 Normal brain development and aging: quantitative analysis at in vivo MR imaging in healthy volunteers. *Radiology* 216:672–682
9. Giedd JN, Blumenthal J, Jeffries NO, Castellanos FX, Liu H, Zijdenbos A, Paus T, Evans AC, Rapoport JL 1999 Brain development during childhood and adolescence: a longitudinal MRI study. *Nat Neurosci* 2:861–863
10. Pfefferbaum A, Mathalon DH, Sullivan EV, Rawles JM, Zipursky RB, Lim KO 1994 A quantitative magnetic resonance imaging study of changes in brain morphology from infancy to late adulthood. *Arch Neurol* 51:874–887
11. Hüppi PS, Warfield S, Kikinis R, Barnes PD, Zientara GP, Jolesz FA, Tsuji MK, Volpe JJ 1998 Quantitative magnetic resonance imaging of brain development in premature and mature newborns. *Ann Neurol* 43:224–235
12. Matsuzawa J, Matsui M, Konishi T, Noguchi K, Gur RC, Bilker W, Miyawaki T 2001 Age-related volumetric changes of brain gray and white matter in healthy infants and children. *Cereb Cortex* 11:335–342
13. Huttenlocher PR, Dabholkar AS 1997 Regional differences in synaptogenesis in human cerebral cortex. *J Comp Neurol* 387:167–178
14. Glantz LA, Gilmore JH, Hamer RM, Lieberman JA, Jarskog LF 2007 Synaptophysin and postsynaptic density protein 95 in the human prefrontal cortex from mid-gestation into early adulthood. *Neuroscience* 149:582–591
15. Dietrich RB, Bradley WG, Zaragoza EJ, Otto RJ, Taira RK, Wilson GH, Kangaroo H 1988 MR evaluation of early myelination patterns in normal and developmentally delayed infants. *AJR Am J Roentgenol* 150:889–896
16. Benes FM, Turtle M, Khan Y, Farol P 1994 Myelination of a key relay zone in the hippocampal formation occurs in the human brain during childhood, adolescence, and adulthood. *Arch Gen Psychiatry* 51:477–484
17. Saksena S, Husain N, Malik GK, Trivedi R, Sarma M, Rathore RS, Pandey CM, Gupta RK 2008 Comparative evaluation of the cerebral and cerebellar white matter development in pediatric age group using quantitative diffusion tensor imaging. *Cerebellum* 7:392–400
18. Steinlin M 2008 Cerebellar disorders in childhood: cognitive problems. *Cerebellum* 7:607–610
19. Rapoport M, van Reekum R, Mayberg H 2000 The role of the cerebellum in cognition and behavior: a selective review. *J Neuropsychiatry Clin Neurosci* 12:193–198
20. Schmahmann JD, Sherman JC 1998 The cerebellar cognitive affective syndrome. *Brain* 121:561–579